Journal of
NANOSTRUCTURES

Numerical Investigation of Nanofluid Mixed Convection and Entropy Generation in an Inclined Ventilating Cavity

H. Khorasanizadeh[a],*, J. Amani[b], M. Nikfar[a], M. Hemmat[c]

[a]*Faculty of Mechanical Engineering, University of Kashan, Kashan, Iran*
[b]*Faculty of Mechanical Engineering, Isfahan University of Technology, Isfahan, Iran*
[c]*Department of Mechanical Engineering, University of Semnan, Semnan, Iran*

*Corresponding author:
E−mail address:
khorasan@kashanu.ac.ir
Phone: *+98 361 5912449*
Fax: *+98 361 5912424*

Abstract

This paper presents results of a numerical study of mixed convection and entropy generation of Cu–water nanofluid in a square ventilating cavity at different inclination angles. Except a piece of bottom wall with a uniform heat flux, all of the cavity walls are insulated. The inlet port is placed at the bottom of the left wall and the outlet port is positioned at the top of the right wall. Entropy generation, Bejan number, average Nusselt number and heat source temperature have been investigated for Richardson numbers between 0.1 and 10, Reynolds numbers in the range of 1 and 300, solid volume fractions between 0 and 0.06 and cavity inclination angles between −90$^\mathrm{o}$ and 90$^\mathrm{o}$. The results show that the average Nusselt number increases with increasing Richardson number for cavity inclination angle of 30$^\mathrm{o}$, 60$^\mathrm{o}$ and 90$^\mathrm{o}$ but decreases with increasing Richardson number for inclination angle of −30$^\mathrm{o}$, −60$^\mathrm{o}$ and −90$^\mathrm{o}$. Total entropy generation and entropy generation due to heat transfer decreases with increasing Richardson and Reynolds numbers, but the Bejan number increases with increasing Reynolds and Richardson numbers.

1. Introduction

Combined natural and forced convection, commonly called mixed convection, is used in solar energy storage, heat exchanger, lubrication technology, electronic equipment cooling, and heating and drying processes. A serious limitation for development of energy−efficient heat transfer is low thermal conductivity of conventional fluids such as water, ethylene glycol and etc. An innovative technique to improve the heat transfer is use of nanofluids. The subjects of addition of nanoparticles to the base fluid and the effective thermal conductivity and viscosity of nanofluids obtained have been topics of intensive analytical, numerical and experimental investigations [1−7].

By investigating the physical, geometric and the total entropy generation of processes, researchers can design systems with minimum loss of available energy and enhance the thermal performance of the systems. For natural convection heat transfer, many investigations on the local and total entropy generation of conventional fluids in variety of geometries have been done so far [8−12]. For mixed convection, Tasnim and Mahmoud [13] focused on the nature of irreversibility analysis inside a vertical cylindrical annulus based on entropy generation. They derived an analytical expression for the velocity and temperature which essentially expedite to obtain expressions for local and average entropy. Further entropy generation minimization analysis was performed to calculate the optimum radius ratio and a correlation was proposed. Boulama et al. [14] investigated the steady−state, laminar and fully developed mixed convection of a binary non−reacting gas mixture flowing upward in a vertical parallel−plate channel, analytically. Ben Mansour et al. [15] obtained explicit analytical expressions for the temperature and velocity profiles as well as for

the axial pressure gradient in a vertical tube. Chen et al. [16] numerically investigated the entropy generation, irreversibility factor and Bejan number in mixed convection.

Due to practical importance, the heat transfer characteristics of nanofluids mixed convection within tubes or driven lid enclosures have been subjects of some other studies [17−20]. Steady laminar forced convection inside a square cavity with inlet and outlet ports for different location and width of the ports was studied by Saeidi and Khodadadi [21] using a finite−volume−based computational method. Shahi et al. [22] also studied mixed convection flows of Cu−water nanofluid in a square cavity with inlet and outlet ports numerically.

Entropy generation of nanofluid mixed convection within a square cavity with inlet and outlet ports has not been subject of any study yet. In this study a square cavity having a uniform flux heat source placed on the bottom wall, similar to the geometry of Saeidi and Khodadadi [21] and Shahi et al. [22], has been considered but unlike them different inclination angles of the cavity has been considered. The effects of volume fraction of nanoparticles, inclination angle, Re and Ri on the details of the flow, the average Nusselt number, entropy generation and temperature distribution on the heat source surface have been investigated.

2. Problem statement and boundary conditions

The geometrical configuration of the two−dimensional square ventilated cavity considered in this study is shown schematically in Fig.1. A uniform heat flux section is embedded on the bottom wall. The cavity is subjected to ventilation of Cu-water nanofluid. The inclination angle of the cavity is measured with the angle of bottom wall with horizontal,

and CCW rotation of the cavity is assumed positive. The Prandtl number of base fluid (water) is assumed to be 6.7. Thermo−physical properties of the nanoparticles and the base fluid are shown in Table 1.
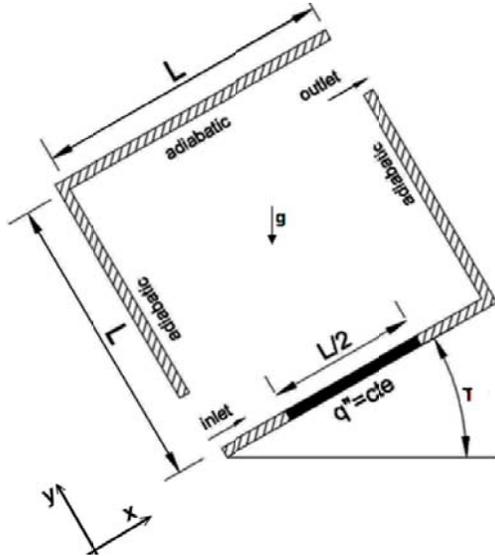
Fig. 1. Schematic of the cavity.

It is assumed that the base fluid and the nanoparticles are in thermal equilibrium and there is no slip between them. All nanofluid properties except density are assumed to be constant and the density of the nanofluid is approximated by the Boussinesq model. All walls are assumed to be insulated except the heat source surface with dimensionless length equal to 0.5, located in the center of the bottom wall. The cold fluid with temperature T_c enters the cavity from the bottom of the left insulated wall and the exit is from the top of the right insulated wall. The inlet and outlet ports have the dimensionless height of L/10.

Table 1. Thermo−physical properties of base fluid and nanoparticles.

Physical properties	Fluid phase (Water)	Solid (Cu)
c_P(J/kg-K)	4179	383
ρ (kg/m^3)	997.1	8954
k (W/m-K)	0.6	400
$\beta \times 10^5$ (1/K)	21	1.67

3. Mathematical formulation

The dimensionless parameters are:

$$X = \frac{x}{L}, \quad Y = \frac{y}{L}, \quad V = \frac{v}{U_0}, \quad U = \frac{u}{U_0}, \quad \Delta T = \frac{q''L}{k_f},$$

$$\theta = \frac{T - T_c}{\Delta T}, \quad P = \frac{p}{\rho_{nf} U_0^2} \tag{1}$$

The dimensionless form of the governing equations are:

$$\frac{\partial U}{\partial X} + \frac{\partial V}{\partial Y} = 0 \tag{2}$$

$$U\frac{\partial U}{\partial X} + V\frac{\partial U}{\partial Y} = -\frac{\partial P}{\partial X} + \frac{\upsilon_{nf}}{\upsilon_f}\frac{1}{\text{Re}}.\nabla^2 U +$$
$$Ri.\frac{(\rho\beta)_{nf}}{\rho_{nf}\beta_f}\theta.\sin(\gamma) \tag{3}$$

$$U\frac{\partial V}{\partial X} + V\frac{\partial V}{\partial Y} = -\frac{\partial P}{\partial Y} + \frac{\upsilon_{nf}}{\upsilon_f}\frac{1}{\text{Re}}.\nabla^2 V +$$
$$Ri.\frac{(\rho\beta)_{nf}}{\rho_{nf}\beta_f}\theta.\cos(\gamma) \tag{4}$$

According to Bejan [23], the volumetric entropy generation rate within a two−dimensional flow in dimensionless form, assuming $T_0 = T_c$, is:

$$S'''_{gen} = S'''_{gen,h} + S'''_{gen,v} =$$
$$\frac{k_{nf}}{k_f}\left[\left(\frac{\partial\theta}{\partial X}\right)^2 + \left(\frac{\partial\theta}{\partial Y}\right)^2\right] + \chi \times$$
$$\left[2\left(\frac{\partial U}{\partial X}\right)^2 + 2\left(\frac{\partial V}{\partial Y}\right)^2 + \left(\frac{\partial U}{\partial Y} + \frac{\partial V}{\partial X}\right)^2\right] \tag{5}$$

The terms $S'''_{gen,h}$ and $S'''_{gen,v}$ represent the entropy generation due to heat transfer and viscous effects of the fluid, respectively, at a given control volume.

The dimensionless entropy generation and irreversibility factor, χ, are defined respectively, as:

$$S'''_{gen} = s'''_{gen} \frac{T_0^2 L^2}{k_f \Delta T^2},$$

$$\chi = \frac{\mu_{nf} U_0^2 T_0 k_f}{q''^2 L^2} = \frac{\mu_{nf} T_0 g^2 \beta_f^2 L^4}{Ri^2 k_f \, Re^2 \, v_f^2} \qquad (6)$$

The total entropy generation due to heat transfer ($S_{gen,h}$) is determined by integrating $S'''_{gen,h}$ inside the cavity, as:

$$S_{gen,h} = \int_0^1 \int_0^1 S'''_{gen,h} dX dY \qquad (7)$$

Similar integration of $S'''_{gen,v}$ is performed to obtain the total entropy generation due to viscous effect ($S_{gen,v}$). The total dimensionless entropy generation (ST) is summation of $S_{gen,h}$ and $S_{gen,v}$.

Bejan number is defined as the dimensionless entropy generation due to heat transfer divided by the total entropy generation expressed as:

$$Be = \frac{S_{gen,h}}{S_T} \qquad (8)$$

Thermal diffusivity and the effective density of the nanofluid, respectively, are given as:

$$\alpha_{nf} = \frac{k_{nf}}{(\rho c_p)_{nf}} \qquad (9)$$

$$\rho_{nf} = \varphi \rho_s + (1-\varphi)\rho_f \qquad (10)$$

The heat capacitance and the thermal expansion coefficient of the nanofluid, respectively, are:

$$(\rho c_p)_{nf} = \varphi(\rho c_p)_s + (1-\varphi)(\rho c_p)_f \qquad (11)$$

$$(\rho\beta)_{nf} = \varphi(\rho\beta)_s + (1-\varphi)(\rho\beta)_f \qquad (12)$$

The viscosity of the nanofluid is estimated using the Brinkman model given by [2]:

$$\mu_{nf} = \frac{\mu_f}{(1-\varphi)^{2.5}} \qquad (13)$$

The effective thermal conductivity of the nanofluid is approximated by the Maxwell–Garnetts model [3] expressed by:

$$\frac{k_{nf}}{k_f} = \frac{k_s + 2k_f - 2\varphi(k_f - k_s)}{k_s + 2k_f + \varphi(k_f - k_s)} \qquad (14)$$

The local Nusselt number and the average Nusselt number on the heat source surface, respectively, are:

$$Nu = \frac{hL}{k_f} = \frac{1}{\theta(x)} \qquad (15)$$

$$Nu_m = \frac{1}{L/2} \int_{\frac{L}{4}}^{\frac{3L}{4}} Nu dx \qquad (16)$$

The boundary conditions are:

Vertical walls:
$$\begin{cases} U = V = 0 \\ \dfrac{\partial \theta}{\partial X} = 0 \end{cases}$$

Top wall and insulated parts of bottom wall:
$$\begin{cases} U = V = 0 \\ \dfrac{\partial \theta}{\partial Y} = 0 \end{cases}$$

Heat source:
$$\begin{cases} U = V = 0 \\ \dfrac{\partial \theta}{\partial Y} = -\dfrac{k_f}{k_{nf}} \end{cases} \qquad (17)$$

Inlet port:
$$\begin{cases} U = 1, \ V = 0 \\ \theta = 0 \end{cases}$$

Outlet port:
$$\begin{cases} \dfrac{\partial U}{\partial X} = 0, \ V = 0 \\ \dfrac{\partial \theta}{\partial X} = 0 \end{cases}$$

4. Numerical method

The continuity, momentum and energy balance equations have been solved through a control−volume formulation given by Patankar [24]. The SIMPLE algorithm has been used for the pressure velocity coupling. To study the effect of the grid size on the results, a complete study was performed on the number of grid points in uniform mesh. The results of this study for two cases are shown in Table 2. Variation of the Nu_m and total entropy generation by varying the number of meshes show that 181×181 meshes are sufficient.

In order to validate the numerical results, the entropy generation, the Be number and Nu_m

number were obtained for a cavity problem similar to the study of Oliveski et al. [11] for various constant irreversibility factors. Comparison of results, presented in Table 3, reveals good agreement.

Table 2. Effect of grid size on Nu_m and total entropy generation for two particular cases.

Number of grids	Ri=10.0, Re=50, φ=0.02, γ=0.0^o		Ri=5.0, Re=1, φ=0.06, γ=30°	
	Nu_m	S_T	Nu_m	S_T
151×151	12.356	6.27e−4	4.36	1.868
171×171	12.356	6.28e−4	4.72	1.919
181×181	12.356	6.32e−4	4.92	1.946
191×191	12.356	6.33e−4	5.03	1.954

Table 3. Comparison of results obtained in this study* with those of Oliveski et al. [11]**.

Ra	χ	S_T	Be	Nu_m	
10^5	10^{-4}	23.172	0.196	4.667	*
		23.87	0.183	4.531	**
10^3	10^{-4}	1.153	0.9701	1.118	*
		1.16	0.96	1.116	**

5. Results and discussion

In this section, results are presented for a parametric study executed for Ri between 0.1 and 10, Re in the range of 1 and 300, φ between 0 and 0.06 and γ between −90° and 90°. The effects of these parameters on flow pattern, Nusselt number, heat source temperature, entropy generation and Bejan number are investigated and discussed.

5. 1. Flow pattern

Due to page restrictions it is not possible to present the streamlines, thus a brief description of the flow field is presented here. When Ri approaches zero, forced convection dominates and natural convection is not important. For this condition and when Re has low value, the velocity of nanofluid entering the cavity is low and as it expands inside the cavity the velocity decreases further. For small values of Re and Ri,

the flow passes through the cavity without any vortexes being created and the streamlines for pure fluid and nanofluid with nanoparticles volume fractions of 0.06 are almost overlapped. For these cases, by changing γ from negative values to zero, stream lines remain unchanged. But change of γ from zero to 60° increases the values of the streamlines near the heat source surface.

The buoyancy force created by heat transfer from heat source to nanofluid causes the fluid to move upward. Its movement is somehow opposite to inlet fluid at the negative angles while assisting it at positive angles. Therefore, at Re= 300 and for γ=−60° two vortexes are created for both Ri=0.1 and 10. Change of γ from −60° to 0° and then to 60°, causes the bottom right clockwise cell to weaken and in some cases to disappear. Also the size of the left counterclockwise cell increases. Consequently, the inlet fluid gets close to the surface of the heat source and sweeps the heat source more efficiently and the values of stream lines near the hot surface are increased resulting in enhanced heat transfer. It is noteworthy that at Ri=0.1 buoyancy force is weak, thus the size of the right cell is smaller compared with its size for Ri=10. At Ri=10, the buoyancy force and natural convection heat transfer reaches its maximum value. Thus pesky force for γ <0° and reinforcement force for γ >0° are increased to their maximum values and hence the effect of angle variation becomes more evident.

With increasing Ri at a specific Re number, the buoyancy force increases and mitigates the fluid tendency to move upward. With increasing Ri at γ<0°, the right vortex get stronger and consequently the inlet fluid recedes from the heat source surface. But for γ>0°, the buoyancy induced heated flow inside the cavity and the inlet flow become concurrent, thus the vortex in the right corner of the enclosure shrinks.

5. 2. Average Nusselt number

Fig. 2 shows the variation of Nu_m on heat source surface for inclination angles between -90 and 90°. The Nu_m increases with either Re or φ increment. The rate of change in Nu_m with Re is higher at lower Re numbers. From Fig. 4 it is observed that adding nanoparticles to base fluid enhances Nu_m in all of the cases studied. Two different behaviors are observed for the effect of changing the Ri. The Nu_m decreases by increasing Ri at $\gamma<0^o$ such that the maximum Nu_m reduction occurs at $\gamma=-90^o$. At this angle, the fluid moving upward due to buoyancy force

blockades the inlet flow and causes separation inside the cavity. By changing γ to -30°, the trend for reduction of Nu_m with increasing Ri is continued but with a slower rate compared to $\gamma=-90^o$ or $\gamma=-60^o$. The Nu_m increases by increasing Ri when γ is zero and this increment of Nu_m augments further for $\gamma>0^o$ such that the maximum value for Nu_m is obtained for $\gamma=90^o$. Consequently, to enhance the heat transfer, $\gamma>30^o$ may be used and if low heat transfer is required $\gamma<-30^o$ should be applied.
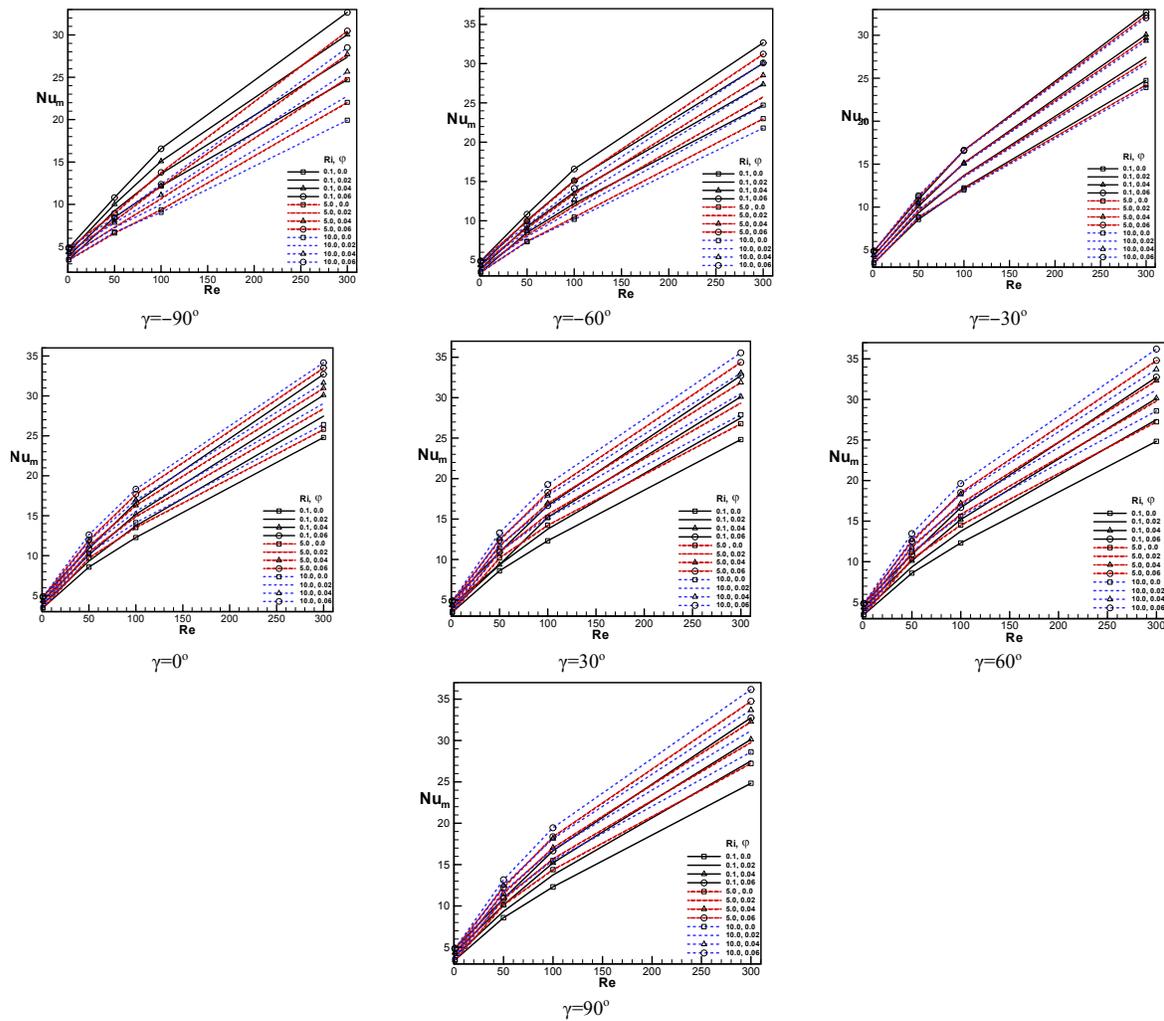
Fig. 2. Variation of Nu_m with Re, Ri, γ and φ.
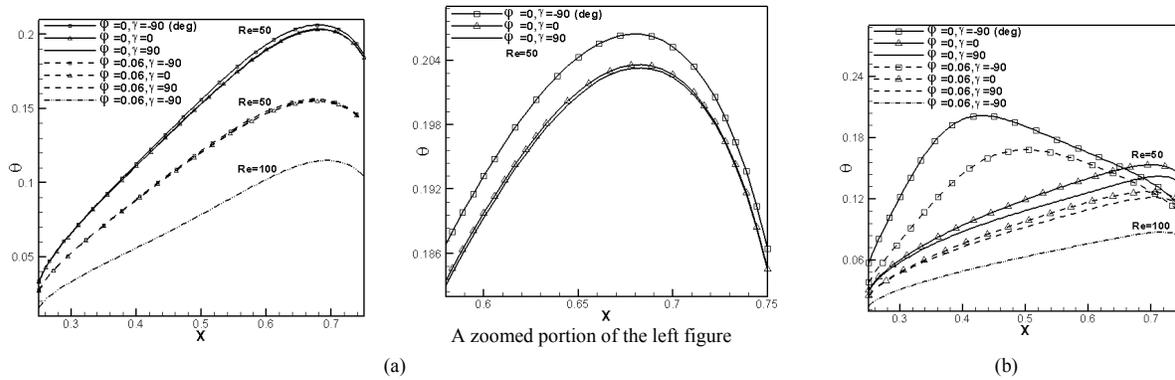
Fig. 3. Temperature distribution on heat source surface, Re=50 and 100, φ=0 and 0.06, γ=−90°, 0° and 90° for (a) Ri=0.1, (b) Ri=10.

5. 3. Heat source temperature distribution

The temperature distribution on the heat source surface is shown in Fig. 3 for Ri of 0.1, 10 and Re of 50 and 100, φ=0 and 0.06 and γ of −90°, 0° and 90°. For Ri=0.1 and for all of the cases studied the temperature on the surface initially rises from left to right and after arriving at a maximum value decreases. The initial increase is due to forced movement of the fluid over the heat source which causes temperature rise for the fluid as well as the heat source surface. The temperature of the heat source is lower when Cu−water nanofluid with φ=0.06 is used. It should be noted that due to lack of buoyancy force at Ri=0.1 the inclination angle does not have effect on the temperature distribution for each particular φ. In other words, the dominant heat transfer mechanism is forced convection. Increase of Re to 100 causes further decrease of heat source temperature due to enhanced forced convection. Separation of flow from the heat source due to the right circulation is the reason for temperature decline after the maximum point. For Ri=10, a similar trend is observed, but the position of the maximum point is taken toward the left. This is due to the bigger size of the right circulation cell because of more buoyancy force at this Ri. It is further seen that

for Re=50 and Ri=10 change of angle from −90° to 0° and then to 90° decreases the heat source temperature. This decline is due to weakening of the right circulation cell when the inclination angle is increased. In other words the buoyancy force does not act opposite to the forced inlet flow anymore.

5. 4. Entropy generation

Entropy generation within the cavity has been studied for all of the cases considered. The total entropy generation is presented in Fig. 4 for different Ri, φ between 0 to 6% and γ=−90°, 0° and 90°. As it can be seen, by increasing Ri or Re, the total entropy generation decreases. It should be noted that in the study of Oliveski et al. [11] constant values for irreversibility factor, χ, have been assumed. In the current study the irreversibility factor is calculated using Eq. (6), by considering variable inlet velocity and variable viscosity of nanofluid, therefore it is not constant. In Eq. (6), χ, has an inverse relation to the square of both Ri and Re. Thus when Ri exceeds one the irreversibility factor decreases sharply, indicating decrease of entropy generation due to viscous effects compared to heat transfer effects. In the other hand increasing Re number causes a lower temperature of heat source surface such that the difference between the fluid temperature and heat source becomes

lower and the entropy generation due to heat transfer decreases. As a result increase of Ri and Re both have positive effects on decreasing the total entropy generation. It should be noted that

the effects of nanoparticle volume fraction and γ could not be seen clearly in Fig. 6, because the vertical axis is in logarithmic scale.
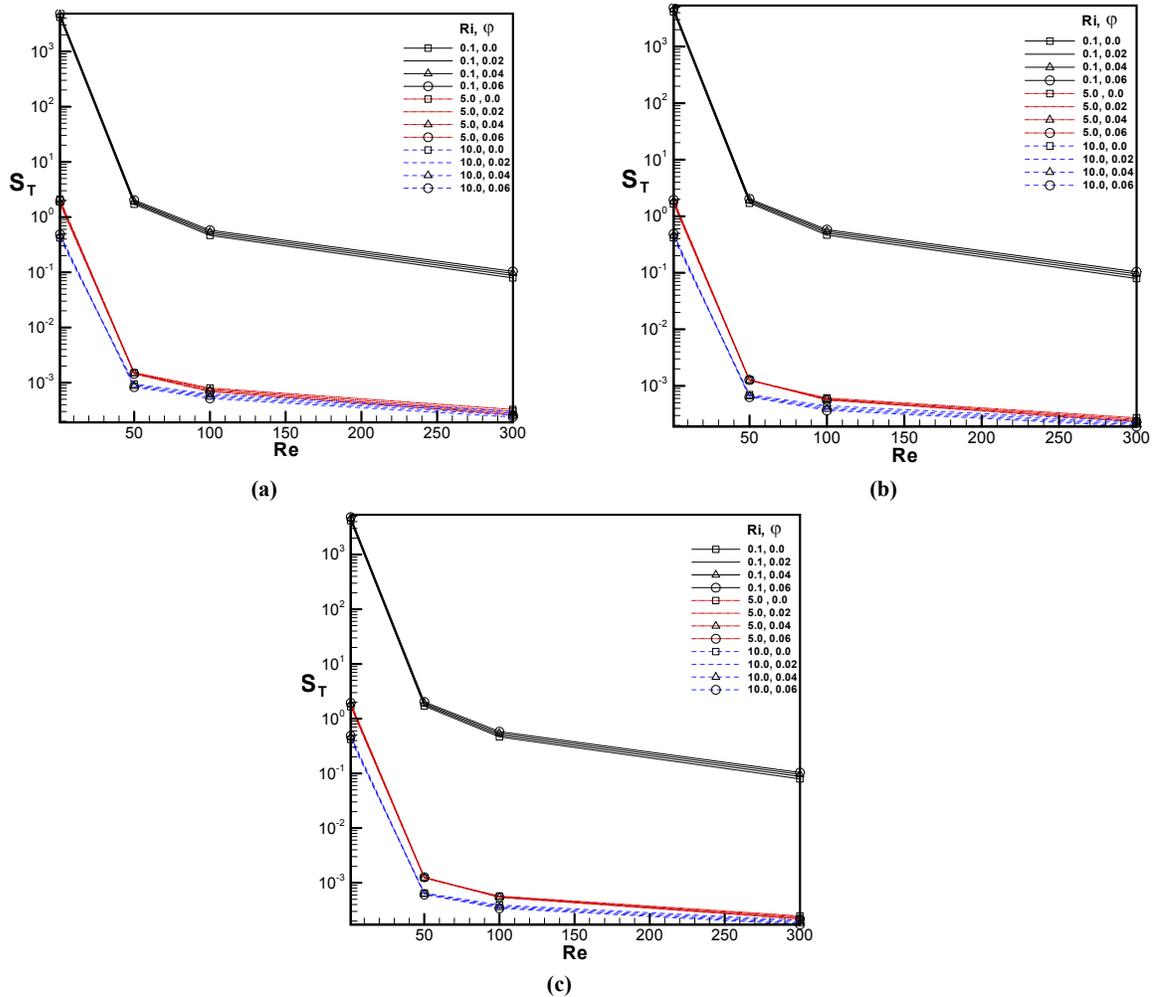
Fig. 4. Total values of entropy generation for (a) γ=−90°, (b) γ=−0° and (c) γ=90°.

5. 5. Bejan number

Variation of Be number with changing other parameters is shown in Fig. 5. The Be number has increased with increasing Re and Ri. For Re=300 the Be number approaches one indicating that the viscous entropy generation is relatively low and the total entropy generation is

solely due to heat transfer effects. If Fig. 4 and 5 are viewed simultaneously it is observed that the lowest value of Be number and highest entropy generation is for Ri=0.1 but the highest Be number and lowest entropy generation is for Ri=10.
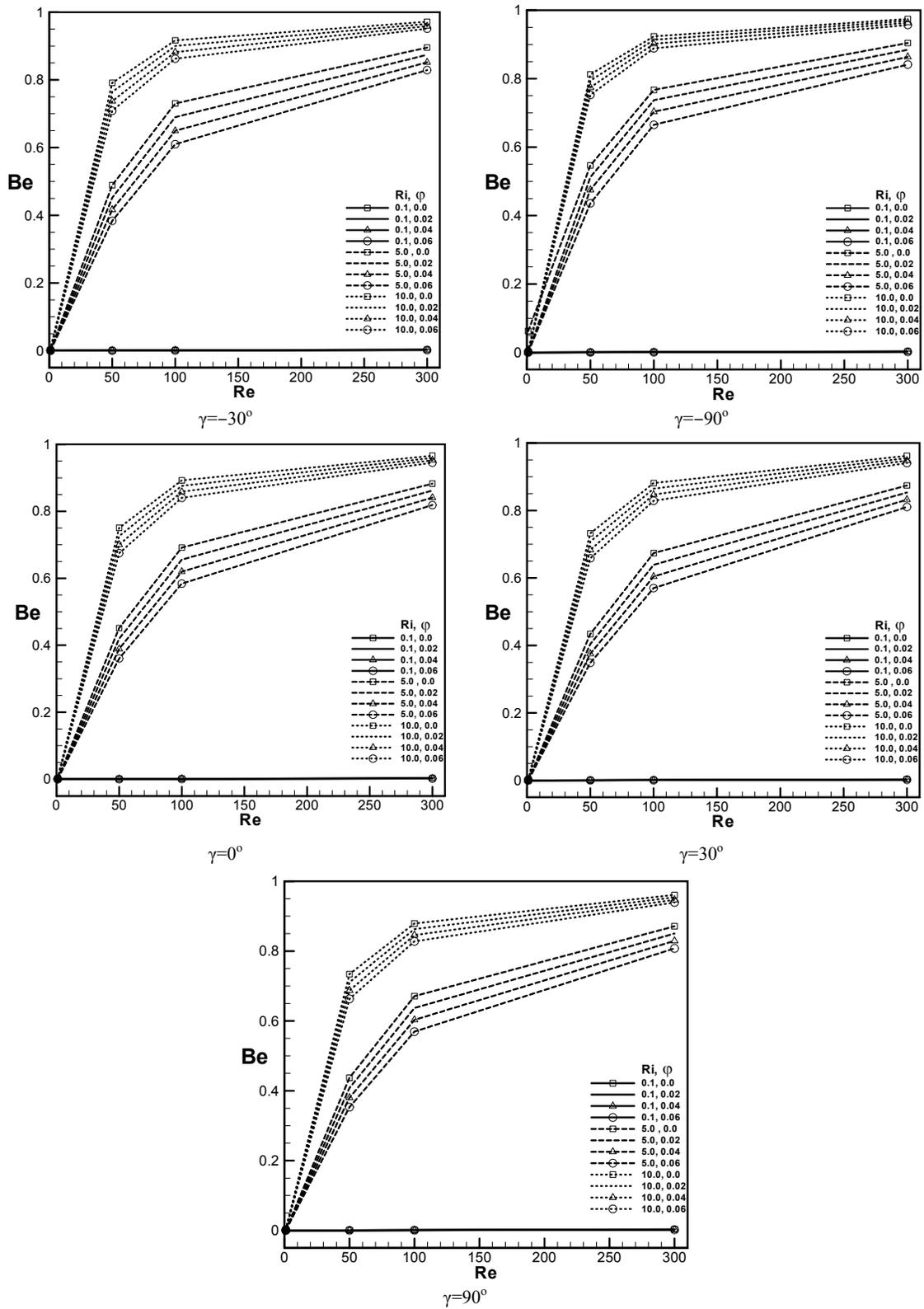
Fig. 5. Bejan number at different γ.

6. Conclusion

In this paper effects of different parameters on mixed convective heat transfer of Cu–water nanofluid in a square ventilating cavity at different inclination angles have been investigated. At Re=100 and 300 and for $\gamma=-60^{o}$ two cells are created inside the cavity for both Ri=0.1 and 10. The Nu_m increases with either Re or φ increment. Also the Nu_m decreases by increasing Ri at $\gamma<0^{o}$. Nu_m increases by increasing Ri when γ is zero and the maximum value of Nu_m is obtained for $\gamma=90^{o}$. By increasing Nu_m, the temperature of heat source surface decreases. To enhance the heat transfer, $\gamma>30^{o}$ may be used and if low heat transfer is required $\gamma<-30^{o}$ should be applied. Total entropy generation and entropy generation due to viscous effects decrease with increasing Ri or Re. Bejan number increases with increasing Re and Ri. For Re=300 it approaches one indicating that the viscous entropy generation is relatively low and the total entropy generation is solely due to heat transfer effects. It is observed that the lowest value of Be and the highest entropy generation is for Ri=0.1 but the highest Be and the lowest entropy generation is for Ri=10.

References

[1]   H. Masuda, A. Ebata, K. Teramae, N. Hishinuma, Netsu Bussei, 4 (1993) 227–233.

[2]   H.C. Brinkman, J. Chem. Phys., 20 (1952) 571–581.

[3]   J.C. Maxwell, A treatise on electricity and magnetism, Second ed., Oxford University Press, Cambridge, 1904, 435–441.

[4]   S.P. Jang, S.U.S. Choi, ASME J. Heat Transf., 129 (2007) 617–623.

[5]   P.K. Namburu, D.P. Kulkarni, D. Misra, D.K. Das, Exp. Therm. fluid Sci., 32 (2007) 397–402.

[6]   H. Chang, C.S. Jwo, C.H. Lo, T.T. Tsung, M.J. Kao, H.M. Lin, Reviews on Advanced Materials Sci., 10 (2005) 128–132.

[7]   C.J. Ho, M.W. Chen, Z.W. Li, Int. J. Heat Mass Transf., 51 (2008) 4506–4516.

[8]   A. Andreozzi, A. Auletta, O. Manca, Int. J. Heat Mass Transf., 49 (2006) 3221–3228.

[9]   M. Magherbi, H. Abbassi, A. Ben Brahim, Int. J. Heat Mass Transf., 46 (2003) 3441–3450.

[10]   Y. Varol, H. F. Oztop, A. Koca, Int. Comm. Heat Mass Transf., 35 (2008) 648–656.

[11]   R.D.C. Oliveski, M.H. Macagnan, J. B. Copetti, Appl. Therm. Eng., 29 (2009) 1417–1425.

[12]   M. Alipanah, P. Hasannasab, S.F. Hosseinizadeh, M. Darbandi, Int. Comm. Heat Mass Transf., 37 (2010) 1388–1395.

[13]   S. H. Tasnim, Sh. Mahmoud, Exergy, an Int. J., 2 (2002) 373–379.

[14]   K. G. Boulama, N. Galanis, J. Orfi, Int. J. Thermal Sci., 45 (2006) 51–59.

[15]   R. Ben Mansour, N. Galanis, C. T. Nguyen, Int. J. Thermal Sci., 45 (2006) 998–1007.

[16]   Ch.K. Chen, H.Y. Lai, Ch.Ch. Liu, Int. Commun. Heat Mass Transf., 38 (2011) 285–290.

[17]   A. Akbarnia, A. Behzadmehr, Appl. Therm. Eng., 27 (2007) 1327–1337.

[18]   S. Mirmasoumi, A. Behzadmehr, Int. J. Heat Fluid Flow, 29 (2008) 557–566.

[19]   M. Muthtamilselvan, P. Kandaswamy, J. Lee, Comm. Nonlinear Sci. Numer. Simul., 15 (2010) 1501–1510.

[20]   F. Talebi, A.H. Mahmoudi, M. Shahi, Int. Comm. Heat Mass Transf., 37 (2010) 79–90.

[21]   S.M. Saeidi, J.M. Khodadadi, Int. J. Heat Mass Transf., 49 (2006) 1896–1906.

[22]   M. Shahi, A.H. Mahmoudi, F. Talebi, Int. Comm. Heat Mass Transf., 37 (2010) 201–213.

[23]   Bejan, Entropy generation minimization, CRC Press, New York, 1995.

[24]   S.V. Patankar, Numerical Heat Transfer and Fluid Flow, Hemisphere Publishing Corporation, Taylor and Francis Group, New York, 1980.